A New Enhanced PSPICE Implementation of the Equivalent Circuit Model of SiPM Detectors

D. Marano, G. Bonanno, S. Garozzo, G. Romeo
INAF – Osservatorio Astrofisico di Catania
Via Santa Sofia 78, I-95123 Catania, Italy
E-mail: dmarano@oact.inaf.it

A. D. Grasso, G. Palumbo, S. Pennisi
DIEEI – Università di Catania
Viale Andrea Doria 6, I-95125 Catania, Italy
E-mail: agrasso@dieei.unict.it

***Abstract* —The present work proposes an improved PSPICE implementation of the equivalent electrical model of silicon photomultipliers (SiPMs) to simulate and predict their transient response to avalanche trigger events. In particular, the developed model provides a detailed investigation of magnitude and timing of the read-out signals and can therefore be exploited to perform reliable circuit-level simulations. The modeling approach used is strictly related to the physics of each basic microcell constituting the SiPM device, and allows the avalanche timing as well as the photodiode current and voltage to be accurately simulated. Predictive capabilities of the proposed model are demonstrated by means of experimental measurements on a real detector. Versatility of the proposed model is also confirmed.**

***Index Terms*—Electrical model, equivalent circuit, PSPICE, output pulse, silicon photomultipliers, transient waveforms.**

I. Introduction

SILICON photomultipliers (SiPMs), also typically referred to as multi-pixel photon counters (MPPCs), are a contemporary class of solid-state detectors which have been gaining great interest and extensive diffusion within the fields of high-energy physics, nuclear medicine, and astrophysics [1]-[11].

SiPMs are constituted by a parallel array of single-photon avalanche photo-diodes (SPADs) connected in parallel and operating above breakdown. When an optical photon strikes one microcell, the related photodiode undergoes a Geiger avalanche and the released charge is collected onto a common electrode. The series quenching resistance integrated in each pixel slows the avalanche current, reducing the voltage drop across the diode terminals. When the current is quenched, the cell begins to recharge, recovering its previous quiescent condition. As a result, the peak amplitude of the SiPM output-generated signal is directly proportional to the total number of microcells which are hit by optical photons.

The availability of an accurate electrical model can enrich understanding of design and behaviour of the SiPM detector as a signal source, allowing a reliable interpretation of its quiescent and transient characteristics and its physical interactions with the coupled read-out electronics.

This work develops a new truthful PSPICE implementation of the electrical model of SiPM sensors based on the peculiar physical features of each SPAD microcell composing the detector structure. Compared to other reported models based on [1], the proposed configuration allows a more accurate representation of the trigger generation process which underlies the SiPM transient response to an incoming avalanche event.

The paper is organized as follows. In Section II the conventional SiPM electrical model is reported. Section III introduces the proposed enhanced model, discussing the improvements of the new PSPICE implementation. Simulation results and comparisons are shown in Section IV. Validation and versatility of the adopted model are addressed in Section V.

II. Conventional SiPM Electrical Model

The circuit electrical model which is typically associated to the elementary SPAD microcell is depicted in Fig. 1. The avalanche photodiode is modeled as a parallel connection between the internal resistance of the diode space-charge region, R_d, and the junction capacitance of the inner depletion layer, C_d. R_q is the quenching resistance, and C_q is its associated stray capacitance, while C_m accounts for metal lines and bonding pads.

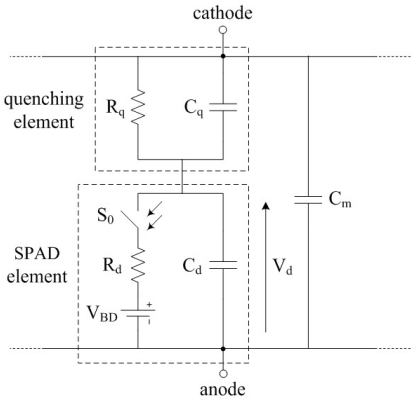

Fig. 1. Traditional equivalent electrical model of a single SPAD microcell.

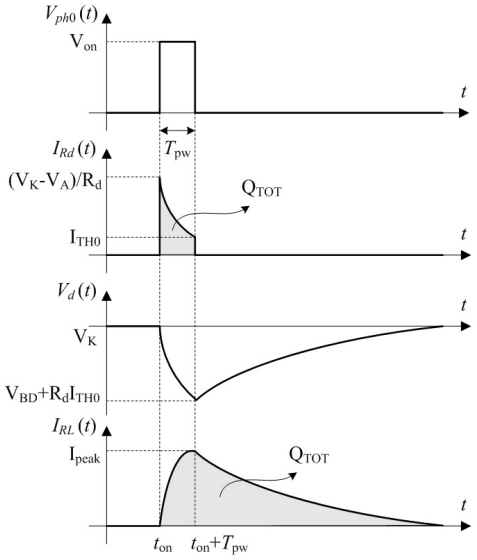

Fig. 2. Characteristic transient current, voltage and output signal waveforms resulting from the traditional SiPM single cell model in Fig. 1.

Avalanche triggering is modeled by means of an ideal DC voltage supply V_{BD} with a series voltage-controlled switch S_0. The switch closes at a preset time t_{on}, demarking the start of a breakdown event, and a pulse current signal is then generated through the photodiode resistance R_d. When this current drops below a predefined threshold value I_{TH0}, the switch opens and the avalanche is quenched. The switch controlling voltage is realized by a square-wave source whose pulse width T_{pw} represents the time between the avalanche triggering time t_{on} and the instant at which the decaying current decreases below the threshold level. Successively, the diode enters the recharging operation, and the transient voltage across its terminals slowly rises towards the external cathode voltage.

The time current and voltage waveforms $i_{Rd}(t)$ and $v_d(t)$, resulting from the SPAD model in Fig. 1 when closed to a load resistor R_L, are illustrated in Fig. 2 with relation to the external step-wise voltage $v_{ph0}(t)$, applied to the control switch and producing the trigger event. The current signal $i_{RL}(t)$ through the output load is also shown.

The main limitation of the conventional trigger generation approach derives from the statistical nature of the avalanche process. More specifically, the aleatory current amplitude I_{TH0} below which the avalanche is not able to self-sustain inevitably involves uncertainty on the choice of T_{pw} as quenching time. As a result, the total charge Q_{TOT} in the avalanche pulse, which is strongly related to the diode quenching time, will be affected by the chosen value of T_{pw}. Most importantly, a constant switch timing in the microcells model does not allow a truthful representation of the output pulse waveforms as a function of the external bias voltage. Indeed, as the overvoltage $V_{OV}=V_K-V_{BD}$ is increased from its nominal value, the potential across the photodiode is initially greater, so that the declining diode current takes a longer time to drop to the quenching level. This entails an increased amplitude of the output pulses during recovery compared to that obtained with constant switching time, with consequent discrepancies on the total pulse charges.

III. Proposed Enhanced Implementation

To overcome the abovementioned limitations and better relate the SiPM electrical model to the physics of the device, an improved circuit configuration is realized to provide an equal switch timing for all bias voltages, hence releasing the diode quenching time from the choice of the pulse width T_{pw} of the switch control voltage.

Fig. 3 shows the simplified block diagram of the improved electrical model of each SiPM basic microcell. A voltage signal V_{ph} starts the trigger avalanche by closing the switch S. A negative feedback loop, including a discriminator D, monitors the diode current and acts upon the switch opening time when this current falls below the specified I_{TH} value.

The novel transient current and voltage waveforms for the improved model in Fig. 3, when closed to a load resistor R_L, are illustrated in Fig. 4. The switch control voltage, V_{ph}, can now be realized as a pulse-wave generator of arbitrary width. However, to perform a correct operation, the voltage pulse is required to have a smaller width compared to the quenching time. As a result of the modified single cell model, although the threshold current level is not sharply defined, the switch S always opens when the photodiode current reaches the constant value of I_{TH} for all operating voltages.

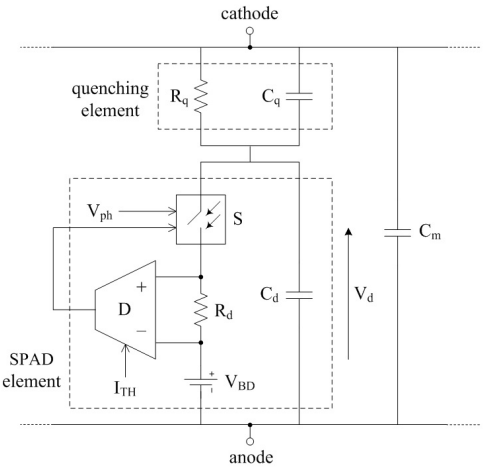

Fig. 3. Simplified block diagram of the improved equivalent electrical model of a single SPAD microcell.

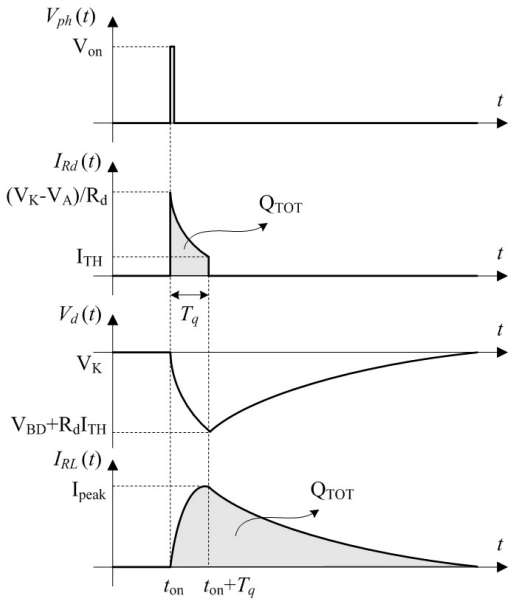

Fig. 4. Characteristic transient current, voltage and output signal waveforms resulting from the improved SiPM single cell model in Fig. 3.

IV. Simulation Results and Comparisons

SPICE circuit implementations of the conventional and improved electrical models in Fig. 1 and Fig. 3 are depicted in Fig. 5, for a number N_f of active pixels over a total number of N microcells. The equivalent electrical model of the remaining N-N_f parallel-connected cells is simply derived by eliminating the circuit branch composed by the V_{BD} voltage source and the photodiode equivalent resistance.

The quenching time of the SiPM output pulses is assumed to be the instant at which the current through the equivalent photodiode resistance $R_{d\_eq}=R_d/N_f$ crosses the threshold level $I_{TH\_eq}=N_f I_{TH}$, established by the average quenching current of an individual microcell and by the number of firing cells.

Referring to the new proposed model in Fig. 5, two parallel voltage-controlled switches, S1 and S2, are exploited in series with the diode resistor and an open-loop operational amplifier is inserted in the feedback branch as a threshold discriminator to sense avalanche current transitions. The initial trigger generation is accomplished by S2 through the input pulse V_{ph}.

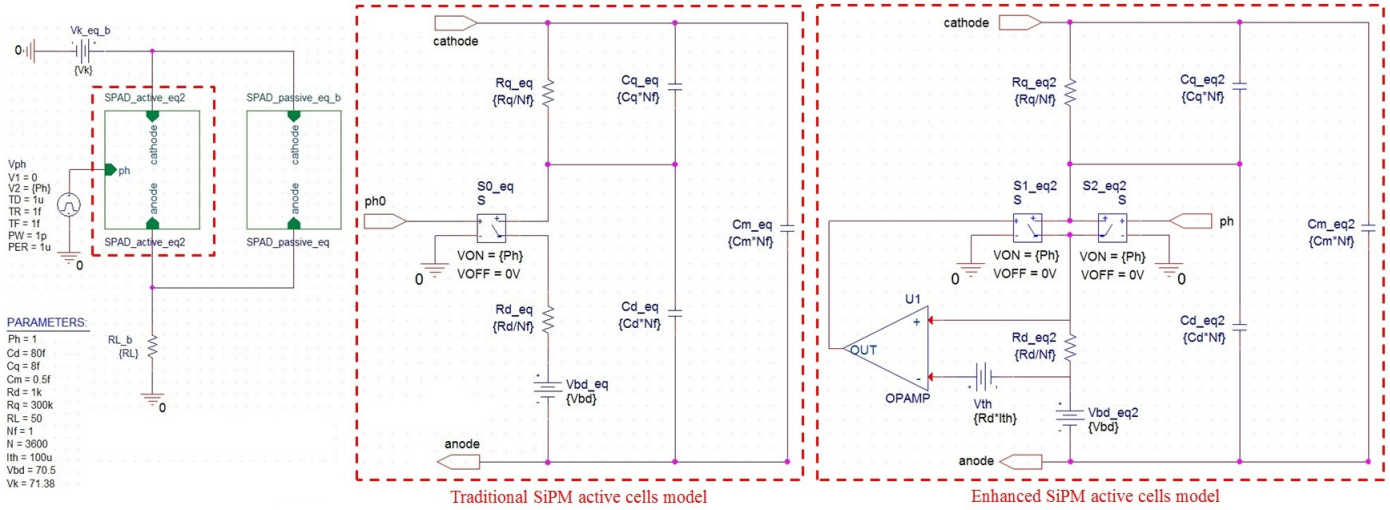

Fig. 5. Schematics of the traditional and enhanced electrical models of the SiPM active cells, and overall SiPM architecture (on the left).

In the steady-state operation, when no trigger events are detected, the voltage across the equivalent diode resistance is lower than the discriminator threshold $V_{TH}=R_dI_{TH}$, so that the negatively-saturated amplifier output voltage opens the switch S1 and no current flows in the circuit. When a positive pulse is applied to V_{ph}, then the avalanche current instantaneously produces a voltage drop on R_{d_eq} which commutates the comparator output towards its positive saturation voltage, hence closing S1 and guaranteeing the discharging current to keep on flowing regardless of S2. As soon as the avalanche current reaches the equivalent threshold level, the discriminator turns again to its preceding state and opens S1, thus collapsing the avalanche and determining the actual quenching time.

Fig. 5 also reports the complete SiPM model (on the left), showing the simulated values of the circuit parameters.

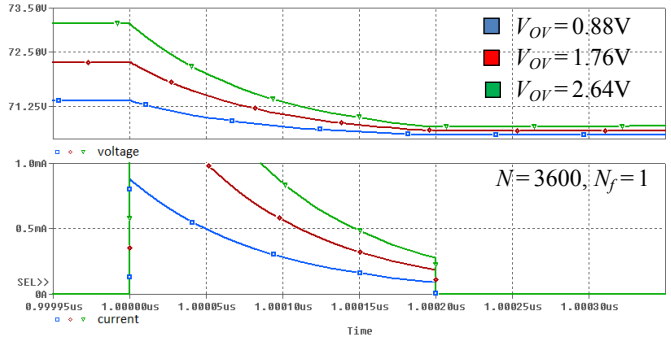

Fig. 6. Transient I_{Rd} and V_d waveforms for the conventional SiPM model.

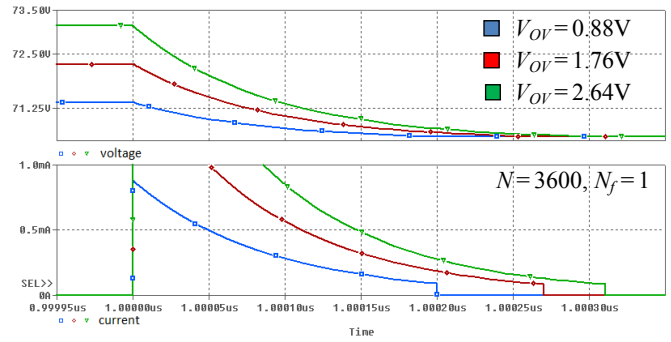

Fig. 7. Transient I_{Rd} and V_d waveforms for the improved SiPM model.

To confirm the different effect of increasing overvoltage on the pulse waveforms of the conventional and improved SiPM electrical models, Fig. 6 and Fig. 7 illustrate, respectively, the voltage across the photodiode and the current through the diode resistance for three rising values of V_{OV}. As can be noted, with a constant switching time, the charge collected from the avalanche pulses does not increase with overvoltage as much as it raises in the improved electrical model. As a result, the amplitude of the SiPM output signal is also found to be slightly greater in the proposed SPICE model, demonstrating a more truthful agreement with the physics of the device.

V. Model Validation and Versatility

To confirm predictive capabilities of the adopted model, experimental measures are carried out on a physical 3×3mm^2 50-µm pitch Hamamatsu device. The detector unit under test is connected to the input of a power/amplification system with a 50-Ω input resistance and a tunable-gain pre-amplifier.

Circuit parameters of the Hamamatsu device are estimated based on experimental measurements and the extracted values are reported in Fig. 5. Parameters extraction is accomplished through a dedicated characterization procedure [10]-[11].

For a single firing cell, data outputs of both simulated and measured output voltage pulses are merged together in Fig. 8 for N=3600, V_{OV}=0.88V, and for a 36-dB pre-amplifier gain. As inspected, the simulated and experimental curves are well-matched, confirming the effectiveness of the adopted model.

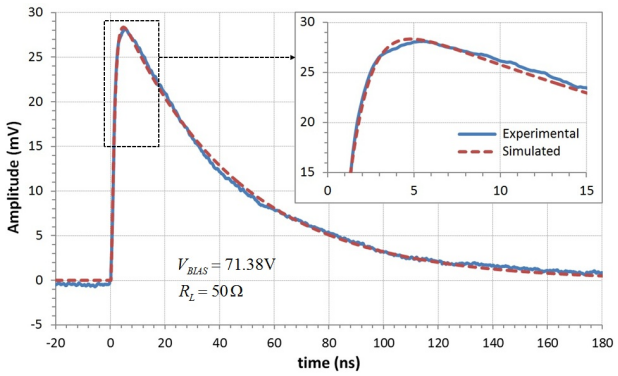

Fig. 8. Simulated and experimental output pulse waveform comparison.

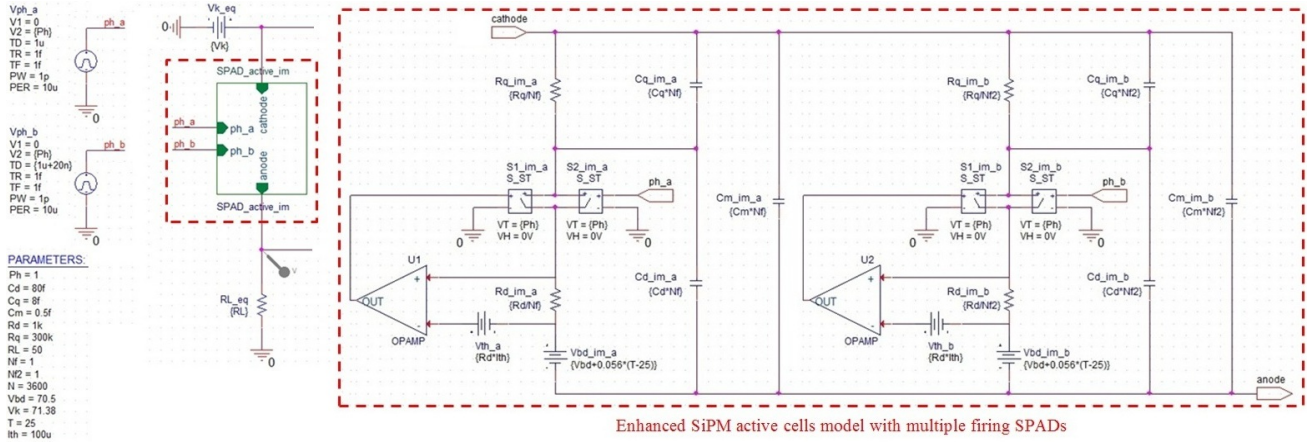

Fig. 9. Schematic of the SiPM active cells model simulating multiple firing cells before complete recovery, and overall SiPM architecture (on the left).

The proposed SiPM model implementation also shows versatility when simulating, after an avalanche trigger in a given SPAD, succeeding ignition events in different cells within the complete recovery of the original avalanche. Fig. 9 depicts the schematic of the modified active cells model, where an additional active branch is introduced to simulate additional firing cells 20ns after the first trigger event.

Moreover, SiPM afterpulse or delayed cross-talk effects can be mimicked through the adopted model by means of a proper external stimulus provided to one of the available input pins of the active cells block. Fig. 10 illustrates, for instance, a simple circuit generating two afterpulses after 40ns and 120ns from an original avalanche.

Fig. 11 reports, as an exemplary case, the simulated results of a single-photoelectron (1-pe) pulse signal from the adopted model, followed by two afterpulses and a successive trigger pulse from a second cell fired after 10ns from the last event.

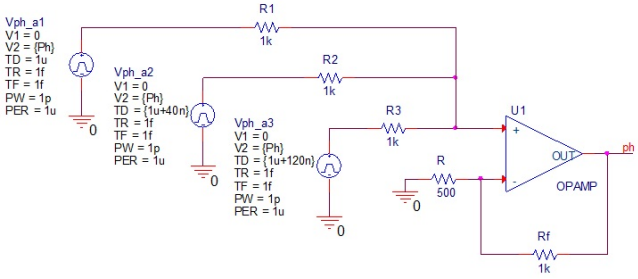

Fig. 10. Schematic of an external stimulus mimicking SiPM afterpulses.

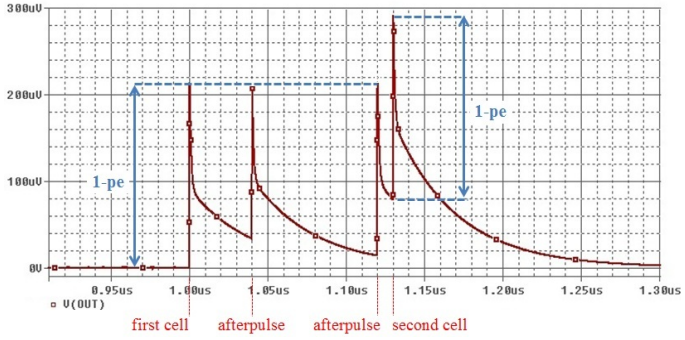

Fig. 11. Transient simulation of a first SiPM cell firing at time t=1µs, followed by two afterpulses and an ensuing trigger event from a second fired cell.

Finally, temperature variations on the breakdown potential can also be accounted for in the adopted model by properly expressing the V_{BD} voltage sources as shown in Fig. 9, where a temperature coefficient of 56mV/°C is assumed.

VI. Conclusions

A new accurate electrical model is developed to simulate, validate, and predict the output response of SiPM detectors. The adopted model allows for an accurate representation of the device behaviour. The trigger avalanche is simulated by means of a pair of parallel voltage-controlled switches, along with a negative feedback loop controlling the current through the photodiode. Model parameters values are extracted based on experimental measurements. The adopted model has been successfully validated and versatility is also confirmed.

References

[1] S. Cova, *et al.*, "Avalanche Photodiodes and Quenching Circuits for Single-photon Detection", *Applied Optics*, pp. 1956-1976, vol. 35, n. 12, 1996.

[2] D. Marano, *et al.*, "Electro-Optical Characterization of MPPC Detectors for the ASTRI Cherenkov Telescope Camera", *Nucl. Instr. and Meth. in Phys. Res. A*, vol. 768, pp. 32-42, 2014.

[3] D. Marano, *et al.*, "Improved SPICE Electrical Model of Silicon Photomultipliers", *Nucl. Instr. and Meth. in Phys. Res. A*, vol. 726, pp. 1-7, 2014.

[4] N. Pavlov, G. Mæhlum, D. Meier, "Gamma Spectroscopy Using a Silicon Photomultiplier and a Scintillator", *Proc. IEEE Nucl. Science Symp. Conf. Record*, pp. 173–180, 2005.

[5] S. Seifert, *et al.*, "Simulation of Silicon Photomultiplier Signals", *IEEE Trans. on Nucl. Science*, vol. 56, no.6, pp. 3726-3733, 2009.

[6] F. Corsi, *et al.*, "Electrical Characterization of Silicon Photomultiplier Detectors for Optimal Front-End Design", *Proc. IEEE Nucl. Science Symp. Conf. Record*, pp. 1276-1280, 2006.

[7] A. K. Jha, H. T. van Damm, M. A. Kupinski, E. Clarkson, "Simulating Silicon Photomultiplier Response to Scintillation Light", *IEEE Trans. on Nucl. Science*, vol. 60, no.1, pp. 336-351, 2013.

[8] D. Marano, *et al.*, "Accurate Analytical Single-Photoelectron Response of Silicon Photomultipliers", *IEEE Sensors Journal*, vol. 14, no. 8, pp. 2749-2754, 2014.

[9] D. Marano, *et al.*, "Silicon Photomultipliers Electrical Model Extensive Analytical Analysis", *IEEE Transactions on Nuclear Science*, vol. 61, no. 1, pp. 23-34, 2013.

[10] G. Bonanno, *et al.*, "Characterization Measurements Methodology and Instrumental Set-up Optimization for new SiPM Detectors - Part I: Electrical Tests", *IEEE Sens. Journal*, vol. 14, no. 10, pp. 3557-3566, 2014.

[11] G. Bonanno, *et al.*, "Characterization Measurements Methodology and Instrumental Set-up Optimization for new SiPM Detectors - Part II: Optical Tests", *IEEE Sens. Journal*, vol. 14, no. 10, pp. 3567-3578, 2014.